HCF Failure Modes and Mechanisms of Dissimilar Welds of Martensite/Austenite Metals at Elevated Temperature

Chendong Shao[1], *Haichao* Cui1, *Fenggui* Lu[1,*], and *Zhuguo* Li[1,**]

[1]Shanghai Key Laboratory of Materials Laser Processing and Modification, School of Materials Science and Engineering, Shanghai Jiao Tong University, Shanghai 200240, PR China

Abstract. In this paper, the high cycle fatigue (HCF) behavior and failure mechanism of welded joint for martensite/austenite dissimilar metals were systematically investigated at elevated temperature. The HCF tests were performed at different elevated temperatures of 550, 600 and 630 ℃ with stress ratio of -1. Most tested specimens failed in the heat affected zone (HAZ) of martensite metal, while minor failure occurred on the weld metal (WM) with comparatively more scattered fatigue life. Fatigue crack in the WM initiated from welding defects like porosities and non-metallic inclusions. For failures in the 10Cr-HAZ, fatigue cracks nucleated from the interior matrix of HAZ, which possessed lower hardness. The initiation of cracks was divided into facet type crack origin (FTCO) and rough type crack origin (RTCO). FTCO was observed for specimens tested at high stress amplitude with fatigue life below 10^7 cycles. Micro-cracks were observed at prior austenite grain boundaries (PAGBs) at high stress level. Micro-cracks preferred to form at martensite lath boundaries and coalesced into macro-crack leading to the formation of RTCO under the condition of lower stress.

1 Introduction

For economic considerations, different materials are usually used in industrial components to maximize their properties. As an efficient way of joining materials, welding technology is being widely employed in recent decades [1]. Welded components are inevitably subjected to complex dynamic load, which may cause fatigue issues. For high cycle fatigue (HCF), cracks usually nucleate from small defects, which are mainly porosities and non-metallic inclusions in the weld seams. Such defects usually act as a stress raiser and induce highly localized irreversible slip deformations for crack formation. Besides, fatigue crack was also reported to nucleate at interior matrix where no pre-existed defect was detected, which is named interior non-defect fatigue crack origin (INFCO) here. According to Chai [2], fatigue crack initiation transited from surface defects, subsurface inclusions to INFCO with decreasing stress amplitude. Zhao et al. [3] reported that INFCO occurred due to large plastic deformation within the bainite lath, leading to the debonding from the adjacent martensite. Generally, the INFCO was generally found in dual phase steel [2, 3] at room temperature, where the two phases are in a stable proportion and different mechanical properties. Dual-phase microstructure also exists in the heat affected zone (HAZ) of a welded joint, which is named inter-critical heat affected zone (IC-HAZ) [4]. Unlike the dual-phase steel, microstructure in the HAZ is high-gradient distributed due to welding heat effect. Both the proportion between microstructure phases and their mechanical properties vary greatly. Failures from

INFCO in the HAZ is also reported for welded joint at elevated temperatures in our previous study [5], but the mechanism was not fully clarified. The purpose of this investigation aims on getting a better understanding on the formation mechanism of INFCO in the HAZ at high temperature.

2 Test materials and experimental methods

The material investigated in this research was a martensite/austenite dissimilarly welded joint fabricated using multi-layer gas tungsten arc welding (GTAW) technology. The martensite base metal (BM) is a 10Cr steel, while the austenite BM is nickel base alloy. Austenite Thermaint rod was used as the filler wire. Schematic of the welded plate is depicted in **Fig. 1** (a). During the GTAW process, the welding current and voltage adopted for each pass were around 250 A and 10.5 V, respectively. The welding speed was 70 mm/min and post-welding heat treatment (PWHT) at 660 ℃ for 45 h was carried out. The yield and ultimate tensile stresses of the welded joint after PWHT are 552 and 744 MPa, respectively.

---

*
Corresponding author: lfg119@sjtu.edu.cn , lizg@sjtu.edu.cn
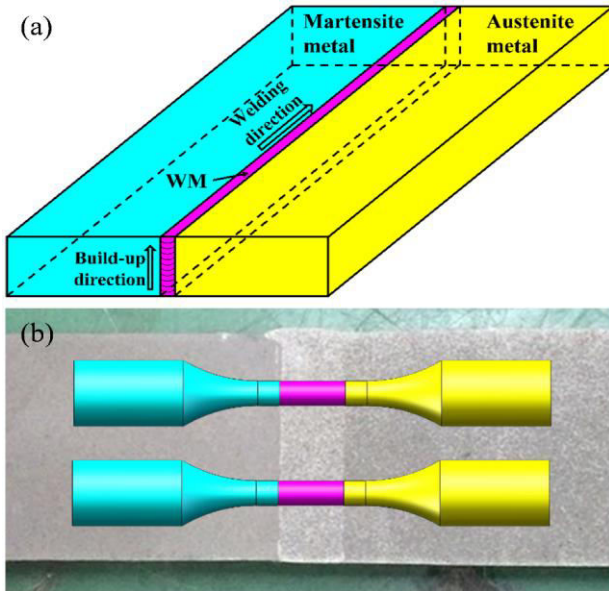
Fig. 1 (a) Schematic of the lump martensite and austenite metal welded by multi-layer GTAW, (b) sampling of high cycle fatigue testing specimens from the welded joint.

High cycle fatigue specimens schematically shown in **Fig. 1** (b) were chipped and machined from the welded joint. The specimens from upper and lower parts were marked and carefully polished. HCF tests were performed following ASTM E466-07 at 550, 600 and 630 ℃. The stress ratio was -1 and the frequency was around 110 Hz. The specimens were heated in an electrical furnace with temperature being controlled within ±1 ℃. Specimens didn`t fracture at $5×10^7$ cycles were terminated as run-outs.

After fatigue test, longitudinal section through the crack initiation region was polished and microstructure of the 10Cr was etched by a solution of $HCl+HNO_3+H_2O$ with volume proportion being 3:5:5. Specific fracture locations were determined by optical microscope and hardness tester. Fracture surfaces were observed by scanning electron microscope and automated digital microscope to reveal the crack initiation site, short crack nucleation and growth morphologies.

3 Results and discussion

3.1 *S-N* curve and failure location

Results of stress amplitude versus fatigue life (*S-N* curves) is presented in **Fig. 2**. Points marked with arrows represent specimens didn`t fracture at $5×10^7$ cycles, namely run-outs. Most specimens failed in the 10Cr-HAZ, and a few in the weld metal (WM). No failure took place in the austenite metal side. It is worth noting that fatigue data of run-outs and failures in WM were excluded when fitting the *S-N* curves of different temperatures in **Fig. 2**.
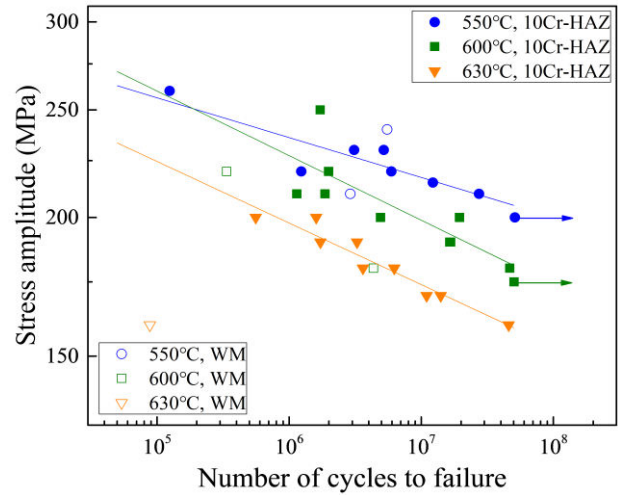
Fig. 2 *S-N* curves for the martensite/austenite dissimilarly welded joint at different temperatures.

It is seen that only five specimens failed in the WM at three testing temperatures. At 550 ℃, two specimens failed in WM with comparable fatigue strength with those fractured in the 10Cr-HAZ. When the temperature increased to 630 ℃, fatigue life of the specimen failed in WM was much lower than that of the failures in 10Cr-HAZ. This indicates that the HCF failures in the WM is more sensitive to temperature increase in this range.
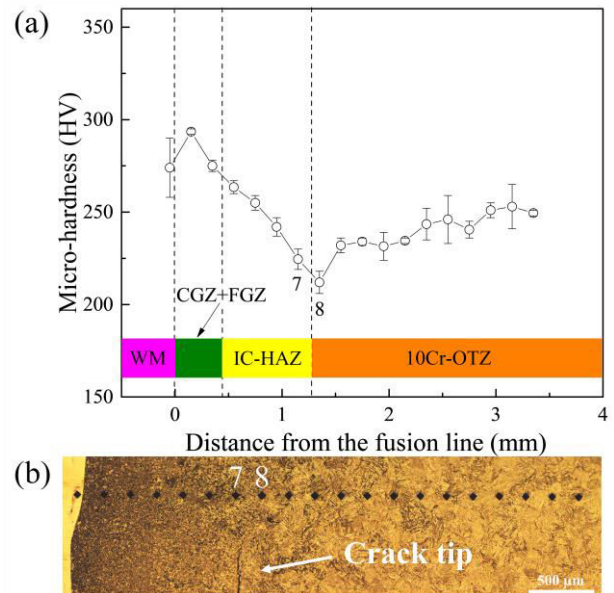
Fig. 3 (a) Micro-hardness distribution across the welded joint, (b) crack location corresponding to the micro-hardness test points.

For failures in the HAZ, the fatigue life is more logarithmically related to the applied stress amplitude and of smaller divergence. Since most failures took place in the 10Cr-HAZ, it is deemed to be the weakest part of the joint at elevated temperatures. With increasing distance from the fusion line, the 10Cr-HAZ consists of several parts, namely coarse grain zone (CGZ), fine grain zone (FGZ), IC-HAZ and over tempered zone (OTZ) as shown in **Fig. 3** (a). For the four zones, the micro-hardness is highest in the CGZ and lowest at the

boundary of the IC-HAZ and OTZ. For 10Cr material, the original microstructure is martensite lath. In the OTZ, the martensite lath was simply tempered during welding. In the IC-HAZ, the microstructure partially austenited during welding and transformed into martensite upon cooling. During the following PWHT process, microstructure in both the OTZ and IC-HAZ was tempered. In such, the microstructure near point 8 is mostly high temperature-tempered martensite (HTTM) with comparatively low strength. In **Fig. 3** (b), the specific failure location of 10Cr-HAZ failures can be determined, as the crack locates between points 7 and 8, where the micro-hardness is lowest in the 10Cr-HAZ, namely lowest hardness zone (LHZ).

3.2 Fracture surface and microstructure observation

Fracture surface of the failed specimens were observed to better understand the crack initiation mechanism. In **Fig. 4** are shown two typical fracture surfaces for failures in the WM. In **Fig. 4** (a), the fatigue crack nucleated from an interior porosity in the WM near the 10Cr-fusion line, and propagated into the 10Cr-HAZ. Crack surface in the WM with austenite microstructure showed obvious crystallographic characteristics, while in the 10Cr-HAZ it is mainly transgranular propagation with coarse fatigue ratcheting marks. The specimen in **Fig. 4** (b) nucleated the crack from a surface non-metallic inclusion with short fatigue life. Combining the previous discussion, it can be concluded that the welding defects are the cause for failures in the WM.
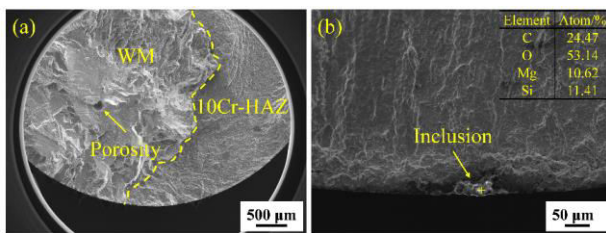
Fig. 4 Fracture surface of specimens failed in the WM, (a) crack initiation from interior porosity in the WM near fusion line of 10Cr side (550℃, 210 MPa, N_f = 2.90×10^6), (b) crack initiation from surface defect in the WM (630℃, 160 MPa, N_f = 8.84×10^4).

For failures in the 10Cr-HAZ, the fracture surface and the microstructure in the LHZ were both observed to better reveal the mechanism. In **Fig. 5** (a) and (b), fatigue crack initiated from a smooth facet at 250MPa and no defect was observed, which is named facet type crack origin (FTCO) in this study. FTCO was only observed in specimens failed with fatigue life below 10^7 cycles. In **Fig. 5** (c) and (d), the crack initiation facet is with an angle of about 45° to the loading direction. After the crack extends into a certain size, it grows perpendicularly to the loading direction in many planes and forms the ratcheting marks shown in **Fig. 5** (a). Microstructure near the fracture surface is presented in **Fig. 6**. Micro-cracks can be observed at prior austenite grain boundary (PAGB) and martensite lath boundaries

(MLBs).
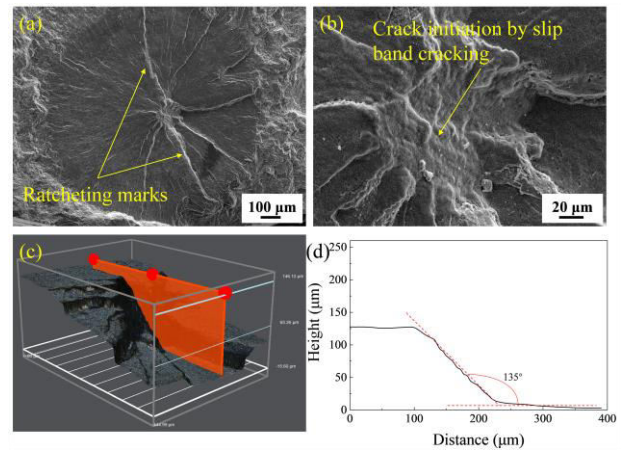
Fig. 5 Facet type crack origin in the 10Cr-LHZ (600℃, 250 MPa, N_f = 1.72×10^6).
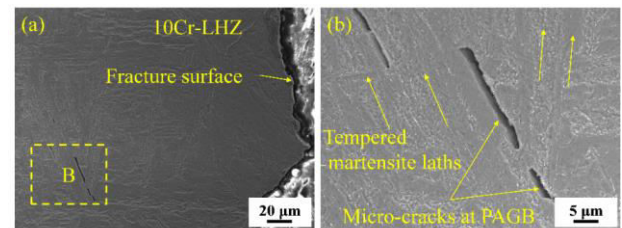
Fig. 6 Micro-cracks observed along prior austenite grain boundary near fracture surface.

For failures with longer fatigue life (>10^7 cycles), typical morphologies of the fracture surfaces are shown in **Fig. 7**. Instead of the smooth facet, the crack initiation site appears quite rough, and is named rough type crack origin (RTCO). Similar rough area named fine granular area (FGA), was reported on defect-induced fracture surface of high strength steels [6] and some weld metals [7]. Generally, rough area indicates extremely slow crack growth rate, and was mostly observed in the very high cycle fatigue regime (VHCF, >10^7 cycles). Different from the FGA, the RTCO in this investigation was not accompanied with defect, and was with an angle to the loading direction, which is similar with the FTCO. In **Fig. 8**, large number of micro-cracks and macro-cracks can be observed along the martensite lath boundaries (MLBs) near the fracture surface.
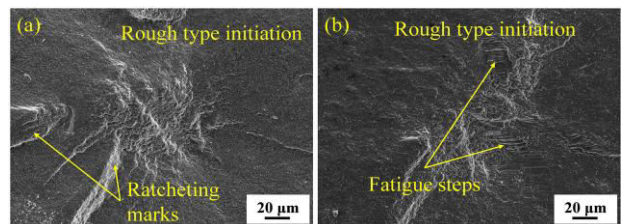
Fig. 7 Rough type crack origin in the 10Cr-LHZ: (a) 550℃, 210 MPa, N_f = 2.74×10^7, (b) 630℃, 160 MPa, N_f = 4.58×10^7.
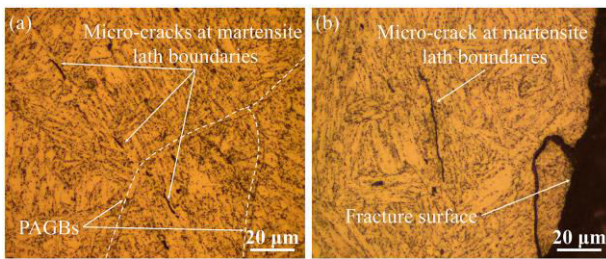
Fig. 8 (a) Micro-cracks and (b) macro-crack observed along martensite lath boundaries near fracture surface.

3.3 Mechanism of different initiation modes

It is previously discussed that the microstructure in the LHZ is mainly HTTM. Due to the locally low strength of the microstructure, resistance property for fatigue crack nucleation is worst in this zone. Under cyclic loading at high temperature, cyclic slip may occur at some preferentially oriented PAGBs and MLBs. At high stress level, micro-cracks can form at PAGBs and extend flat into the size of a prior austenite grain, i.e, the facet in **Fig. 5** (b). Such a large shear crack is hard to be blocked by the surrounding HTTM microstructure and can easily grow into several tension cracks with short fatigue life as shown in **Fig. 5**.

As the stress amplitude getting lower, cyclic slipping is restricted to some local preferential MLBs. With increasing loading cycles and long-term elevated temperature, more and more micro-cracks can form at the MLBs. From the three-dimensional perspective, the formation of RTCO can be a result of the coalescence of adjacent micro-cracks at MLBs in the LHZ. However, this kind of micro-cracks are easier to be captured by the microstructure due to the small size and low stress level, thus leading to longer fatigue life.

4 Conclusion

1. During the HCF testing at elevated temperatures, the austenite microstructure of the WM is more sensitive to welding defects. LHZ of the martensite material is the weakest zone where most HCF failures took place.
2. Failures in the 10Cr-LHZ at elevated temperature nucleated from non-defect matrix with different morphologies, and were named facet type crack origin (FTCO) and rough type crack origin (RTCO).
3. With long-term high temperature and cyclic loading cycles, micro-cracks can form at MLBs and PAGBs in the 10Cr-LHZ. At high stress amplitude, the micro-cracks at PAGBs can extend into FTCO with fatigue life below 10^7 cycles, while micro-cracks at MLBs coalesce to form RTCO with longer fatigue life.

References

1. K. Jeongtea, K. Byeongook, Mater. Sci. Forum, **654-656**, 398-403 (2010)
2. G. Chai, Int. J. Fatigue, **28**, 1533-1539 (2006)
3. P. Zhao, G.H. Gao, R.D.K. Misra, B.Z. Bai, Mater. Sci. Eng. A, **630**, 1-7 (2015)
4. J.A. Francis, W. Mazur, H.K.D.H. Bhadeshia, Mater. Sci. Technol., **22**, 1387-1395 (2006)
5. C. Shao, F. Lu, X. Wang, Y. Ding, Z. Li, J. Mater. Sci. Technol., **33**, 1610-1620 (2017)
6. P. Grad, B. Reuscher, A. Brodyanski, M. Kopnarski, E. Kerscher, Scripta Mater., **67**, 838-841 (2012)
7. M. Zhu, L. Liu, F. Xuan, Int. J. Fatigue, **77**, 166-173 (2015)